Zhang, W, Zou, Z, Wang, J and Du, L

 Multi-ship following operation in ice-covered waters with consideration of inter-ship communication

http://researchonline.ljmu.ac.uk/id/eprint/13289/

Article

Multi-ship following operation in ice-covered waters with consideration of inter-ship communication

Weibin Zhang[a*], Ziyao Zou[a], Jin Wang[b], Lei Du[c]

[a]School of Electronic and Optical Engineering, Nanjing University of Science and Technology, Nanjing 210094, China

[b]Department of Maritime and Mechanical Engineering, Liverpool, Liverpool John Moores University, L3 3AF, UK

[c]Marine Technology, Research Group on Maritime Risk and Safety, School of Engineering, Department of Applied Mechanics, Aalto University, P.O. Box 12200, FI-00076 Aalto, Finland

[*]Corresponding author: Tel +86-13236532288, Email: wbin.zhang@outlook.com

ABSTRACT

With the advancement of technology, the ship-to-ship communication plays an increasingly important role in fleet following operations. In this study, a new ship following model that considers communication conditions is constructed for convoys following icebreaking ships through sea-ice areas. The model combines the effects of ice and communication on speeds and inter-ship distances. Then, the linear stability of the model is analysed. Simulation and analysis using actual data reveal that modelling stability is improved compared to models that do not consider communication and the backward-looking effect. The model provides a theoretical basis for maritime traffic simulation software. Moreover, it can accurately predict changes in the velocities of following ships. Consequently, the high stability of the proposed following model can be utilized for risk mitigation for fleets navigating in ice-covered waters.

KEYWORDS: Internet of vessels; following model; icebreakers; sea-ice; maritime transportation.

1. INTRODUCTION

Maritime transportation in harsh winter sea-ice environments poses specific challenges and only a narrow group of ships is able to navigate independently in ice-covered waters. The remainder of the ships need to be assisted by icebreakers while navigating in frozen sea. The navigation of latter is more complex than the open sea one, and the occurrence likelihood of accidents is higher (Valdez Banda et

al., 2016; Rosenblad, 2007; Zhang and Meng, 2019). Ships led by an icebreaker form a convoy and tend to maintain a constant speed and short distances between themselves. This reduces the risk of becoming stuck in the ice, avoiding ice damages due to ice compression (Kubatet al., 2015; Juurmaaet al., 1998; Kubat et al., 2013; Kubat, 2012). However, at the same time, this increases the risk of collision between the ships in the convoy, which can cause environmental pollution (Zhang et al., 2015; Kim et al., 2017). Therefore the research on safety of arctic navigation has recently gained much attention leading to better understanding of transportation system behaviour and the causes of possible accidents therin (Fu et al., 2018; Zhang et al., 2018; Valdez Banda et al., 2015; Kum and Sahin, 2015).

~~Recent research shows that good training programs can help decrease the risk of oil spills in winter.~~ The experience gained by seafarers during the operation of ships provides an important basis for safe navigation; therefore, it is useful to increase the authenticity of simulated environments and operational procedures. One of the elements of the procedure is good communication between ships in a convoy for increasing navigational safety (Zhang et al., 2019). Some studies have been conducted on the communication system of intelligent ships. With years of experience in communication design, application and verification, some researchers have designed intelligent systems, developed network data exchange protocols, built the information transmission base of smart ships, and successfully applied them to four smart ships. This kind of communication technology covers almost all data types on smart ships, with low delay and high transmission efficiency. It is the basis for the future development of intelligent ships in the field of directed control. Furthermore, based on the integrated navigation technology, four intelligent ships are equipped with intelligent navigation systems, which have the functions of intelligent optimization of route speed, enhanced scope of watchtower, and auxiliary automatic collision avoidance in open waters. In this way, communication technologies were used in the marine traffic to enhance the safety and stability of the ship's navigation (Cheng, 2019; Wang et al., 2019).

However, so far there are no available models of the spatio-temporal patterns of communication between icebreakers and multi-escorted vessels navigating in ice. Such a model could contribute to the improvements in seafarers training and safety of navigation.

In the proposed model, the effects of forward-looking and backward-looking among the leading ship and following ships are taken into consideration. The effect of backward-looking means the crews in the leading ship take into account the following ship's behaviour. The forward-looking means the opposite situation. The proposed model will help improve the stability of fleet navigation and can also be used in applications of simulation software modelling to increase crews' experience of sailing in sea-ice regions.

2. METHODS AND DATA

2.1 The effect of communication on ship following behaviour

Since research into ship following models is lacking, car-following phenomena are often used as an analogy. Usually, a car's following behaviour is determined through its driver's observation of the preceding car's behaviour, mainly by observing its brake lights. However, in ship following scenarios, ships communicate with each other. Therefore, the effect of communication on ship behaviour in convoy navigation should be considered in the ship following models.

Through ship-ship communication basic traffic information can be available and used, such as ships' speeds, positions and courses, and their rates of changes. Thus the changes in the vectors of ship motion parameters due to ships' manoeuvres are communicated among vessels instantly, in comparison with the existing collision avoidance systems, such as ARPA (Automatic Radar Plotting Aid), where it can take up to two minutes for the system to update the information (Bole et al., 2014; Wawruch, 2017). Transmitting navigation information between preceding and following ships allows crews to increase their situational awareness, thus the safety of navigation (Thombre et al., 2015; Ramos et al., 2019).

2.3 The effect of communication on a ship-following model

The optimal sailing speed at the current time is $V(\Delta x_n(t))$, where $\Delta x_n(t)$ represents the distance between ships. The optimal sailing speed is determined by ship speed and distance in the fleet, which is described by Eq. (7). If the current optimal speed is higher than the optimal speed at a previous time, it means that the ship has an acceleration tendency. Similarly, if the optimal speed is lower, it means that the ship tends to decelerate. The optimal speed at a previous time is presented as $V(\Delta x_n(t-\tau))$. Here variable τ is the memory time step. The expression $pV_F(\Delta x_n(t))$ represents the effect of the leading ship to the following ship while $(1-p)V_B(\Delta x_{n-1}(t))$ shows the effect of the following ship to the leading ship. Here p represents the attention given by the current ship's crew to the preceding ship, and $1-p$ represents the degree of influence of the following ship on the current ship.

Peng et al. (2016) proposed an optimal velocity change with memory (OVCM) model. Sun et al. (2012) proposed an optimal velocity model that considers the backward-looking effect or backward-looking and velocity difference (BLVD). Based on these previous studies, the following communication model is defined:

$$C_n = \gamma[V(\Delta x_n(t)) - V(\Delta x_n(t-\tau))]T + pV_F(\Delta x_n(t)) + (1-p)V_B(\Delta x_{n-1}(t)) \tag{1}$$

where the parameter γ is denoted as the intensity of a communication signal via inter-ship communications. $\gamma[V(\Delta x_n(t)) - V(\Delta x_n(t-\tau))]$ is a memory item, which is influenced by the communication condition between the ships. This takes a certain amount of reaction time T. This "memory" represents velocity information and relative data that was already known, then the ship can respond quickly based on known information. γ is the sensitivity coefficient of optimal speed as a function of the memory time step. $V_F(\Delta x_n(t))$ is the optimal speed from forward observation, and $V_B(\Delta x_{n-1}(t))$ represents the optimal speed for backward observation. Thus, C_n is defined as the communication effect on the nth ship.

2.4 Ship convoy operations in sea-ice conditions

When sailing in sea-ice areas, an icebreaker is often needed to open a channel. Other ships follow the icebreaker while maintaining safe distances and speeds (Liikennevirasto, 2017). In this situation, the attempts are made to keep the risk of accidents for a convoy balanced, through the risk assessment (Valdez Banda et al., 2016; Valdez Banda et al., 2015). On one hand the ships are kept on the move, as a result the risk of besetting in ice and resulting ice damage due to ice loads are minimized (Kotilainen et al., 2017; Kujala and Arughadhoss, 2012). On the other hand the risk of collision in a convoy is increased, which can lead to environmental pollution. Numerous operations between ship and icebreaker while navigating in convoy are performed, including ship escort, towing and convoying, as depicted in Figure 1.
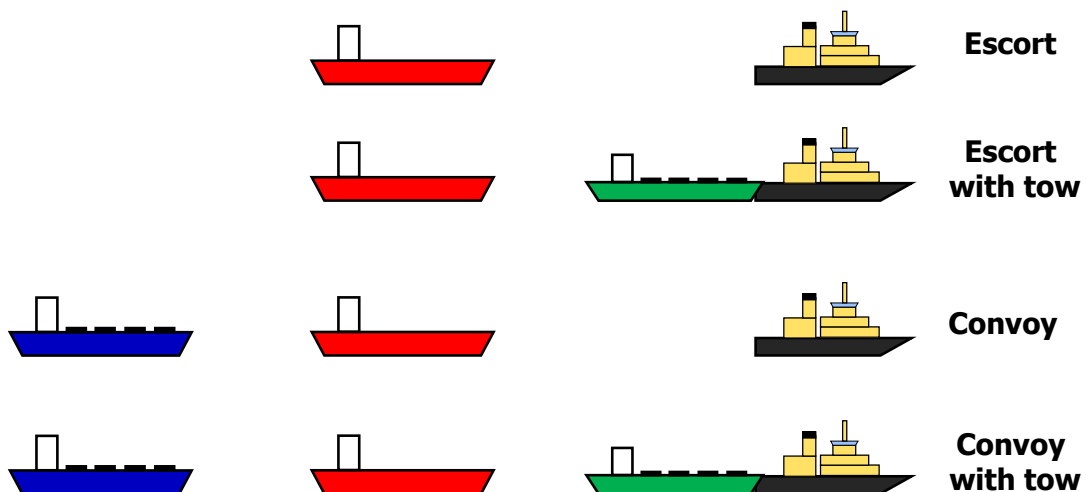
Figure 1. Example of various operations performed by an icebreaker in non-independent navigation mode in winter navigation system (Goerlandt et al., 2017).

In this paper, the safety of multi-ship following operation in ice-covered waters is investigated with consideration given on inter-ship communication and its effect on ship behaviour in ice, through the memory effect. The latter refers to the memory of the crew receiving information, when there is active communication between ships. The crew has the memory information of the previous moment, which can help to adjust the speed of the own ship for the next moment, making the ice navigation safer. Thus the crew's memory governs the ship's speed in the model presented here.

2.5 Maximum speed and safe distance in sea-ice conditions

Maximum speed and safe distance are necessary to calculate the optimal speed of a ship in the fleet, therefore, the following sections explain how to model and compute them.

Safe speed modelling

The navigation speed used in the model, is obtained in a two-step process, comprising big data analysis and maximum speed calculation based on ice numerals.

Big data analysis

First, the regression analysis of big data set comprising ice thickness and resultant navigation speed is performed (Montewka et al., 2019; Montewka et al., 2015). The former is obtained from numerical sea ice model called HELMI (Haapala et al., 2005; Lehtiranta et al., 2012), while the latter is a dataset recorded through the Automatic Identification System (AIS) for a period from 1st to 12th of March 2011 in the Northern Baltic Sea transportation system. The analysed period refers to very harsh winter conditions in the area (Lensu and Kokkonen, 2017; Löptien and Dietze, 2014; Rolf et al., 2018). Since the main interest is in convoy operations involving icebreakers, the traffic data is organized per assisting icebreaker

Maximum safe speed estimation based on ice numerals

The concept of ice numerals is adopted to calculate the maximum safe speed at which a ship can safely navigate in a given ice condition, meaning continuous passage without expecting significant damage to her hull and appendices. Therein the ice numerals (IN) describing the risk of ice navigation in a given ice conditions are determined, as follows:

$$IN = C_a IM_a + C_b IM_b + ... + C_n IM_n \tag{2}$$

where C_i $(i=a,b,..,n)$ represents the concentration in tenths of ice type i, and IM_i represents the ice multiplier for ice type i, as calculated with the use of following formula (each ice includes open water with a value that depends on the ice type):

$$IM = \begin{cases} 2, & 0 \le C < 70 \\ 1, & 70 \le C < 120 \\ -1, & 120 \le C < 151 \end{cases} \tag{3}$$

Here, C is the thickness of the ice with unit of centimeters(cm). The ice multipliers (IM) are calculated according to the Arctic Regime Shipping System (AIRSS), that accounts for ice-class of a ship and prevailing ice concentration and ice types, which are further divided into several categories as. The concentration of sea ice is directly entered into the frame of AIRSS, and the ice thickness is classified according to an ice multiplier. The higher the multiplier value is, the lower the risk of ice-related accidents. The AIRSS ice classification system is shown in Table 1, and the method is explained in detail in (Transport Canada 2018).

Table 1. AIRSS ice multiplier system, (Transport Canada 2018)

Ship category	Ice type				
	Open water	Grey ice	Grey white ice	Thin first-year ice 1st stage	Thin first-year ice 2nd stage
CAC3	2	2	2	2	2
CAC4	2	2	2	2	2
Type A	2	2	2	2	2
Type B	2	2	1	1	1
Type C	2	2	1	1	-1
Type D	2	2	1	-1	-1
Type E	2	1	-1	-1	-1

Figure 2 presents the speed values as obtained from big data (AIS) analysis attributed to the ice numerals as calculated with the use of AIRSS, based on the ice data obtained from the HELMI model. Based on that, the following equation describing the maximum safe speed is obtained (McCallum J,

1996). The equation holds for the ice and operational conditions similar to those encountered during the period covered by the analysed data. This means heavy first year ice conditions, including ice compression and maritime traffic heavily relying on ice breakers assistance.

$$V_{max} = 60.53 IN^3 - 205.4 IN^2 + 228.4 IN - 74.01 \tag{4}$$

where V_{max} is the maximum speed and IN is the ice numerals. This formula is utilized to calculate the allowable speed, that is, the maximum speed at which a ship can safely move in the given ice conditions. Exceeding this speed increases navigational risks.
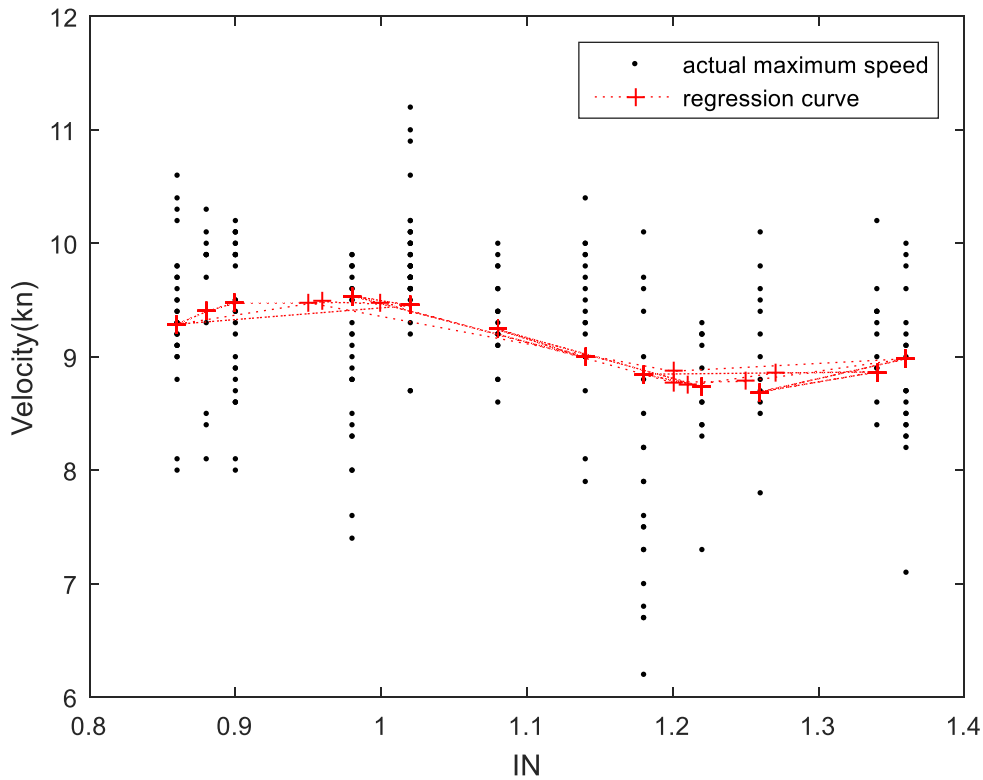

Figure 2. Polynomial regression analysis of safe speed in relation to ice number

Safe distance modelling

To determine the safe distance for ice navigation the following formula is used:

$$D_{safe-ice} = x_p(t_n + \varepsilon) - x_f(t_n + \varepsilon) - l_p - \Delta D \tag{5}$$

7

where, x_p represents the position of the leading ship, x_f represents the position of the following ship, t_n represents the time when the two ships begin to slow down, ε represents the deceleration time interval, l_p represents the length of the hull of the leading ship, and $\Delta D = \alpha \cdot h_{ave} + \beta$ represents the additional distance which vessels aim to maintain between their positions in the convoy, due to the ice conditions (Zhang et al., 2018). Here α and β are coefficients which need to be calibrated on the basis of collected data. The parameter h_{ave} is ice thickness.

3. MODELS

Zhang et al., (2019) have proposed a multiple ship following model. However, some factors were absent in that study, such as communication between ships, the effects of forward-looking and backward-looking, etc. Therefore, an enhanced multiple ship following model under ice conditions is necessary to overcome the shortcoming of the previous study. In order to develop the required enhanced model, three steps are considered. In section 3.1, the behaviour of following ships under communication scenarios is studied. Then in section 3.2, optimal velocity in the ice condition (OVI) model is developed based on the optimal velocity (OV) model by considering the situational awareness of the crew, linking the vigilance with respect to other vessels in convoy and environmental conditions. Finally, in section 3.3, a new multi-ship following model that can be applied to sea-ice environments by considering backward-looking, ice resistant and optimal velocity change with memory (BLI-OVCM) is proposed by combining the effects of the optimal velocity change with the memory (OVCM) model, the backward-looking and velocity difference (BLVD) model and ice conditions.

3.1 Communication scenarios

During heavy winters ice conditions at sea may change rapidly. Thus the best knowledge on the safe routes is possessed by the skilled crew in operating icebreakers. For this reason, during ice navigation some of the burden related to traffic coordination is shifted from the shore-based stations to the icebreakers. The latter are often seen as offshore mobile VTSs (vessel traffic services). Therefore development of a good communication network linking the icebreakers and assisted vessels is crucial for efficient and safe winter navigation. Through the wireless communication the navigation information can be shared between the preceding and following ships. An example of a communication network for an ice convoy is presented in Figure 3. Therein, in a situation where the icebreaker is rapidly brought to a halt (due to environmental or operational reasons), a warning message can be sent to the following

ships. This increases the situational awareness of the officers of the watch on board all ships in a convoy, which significantly contributes to navigational safety (Thombre et al. 2015; Goerlandt et al. 2015; Yim, Kim, and Park 2018), allowing early and safe action to avoid collision. Thus, communication greatly improves the efficiency and safety of navigation in ice convoys.
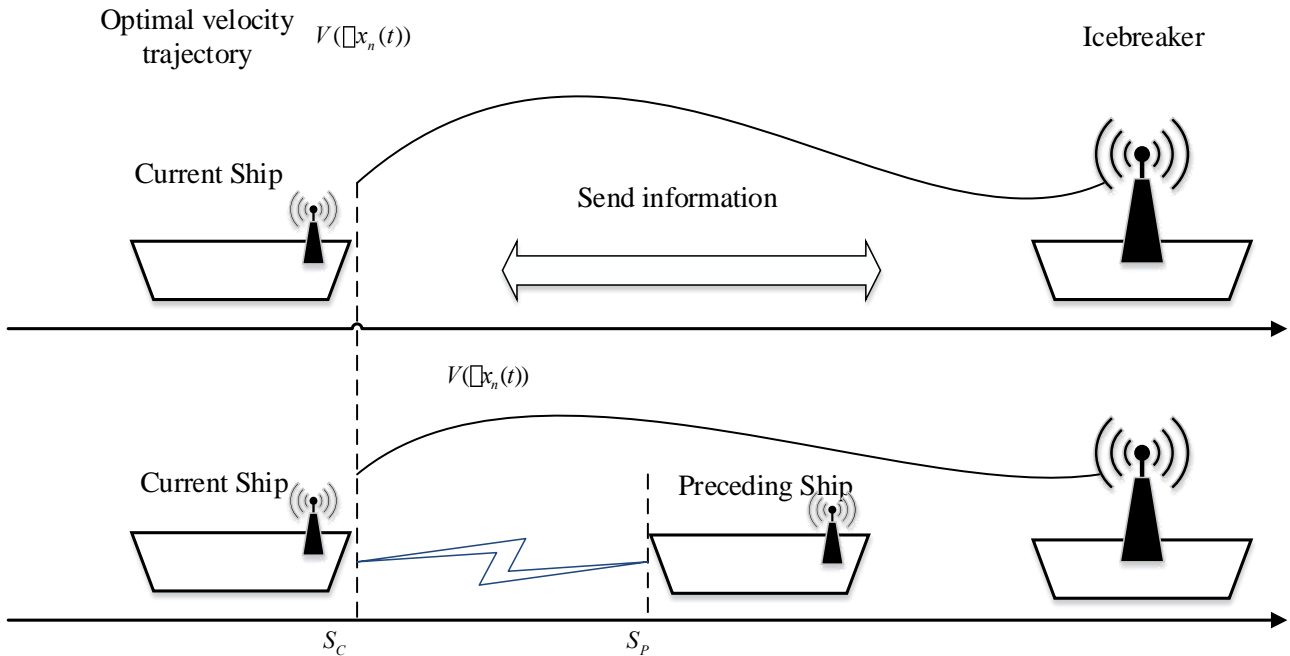

Figure 3. Schematic of ships sailing as part of a communication network

Generally, the ships' navigation is constrained by the safe speed and safe distance allowable in ice-covered waters. A flowchart of a following ship's navigation system is shown in Figure 4.
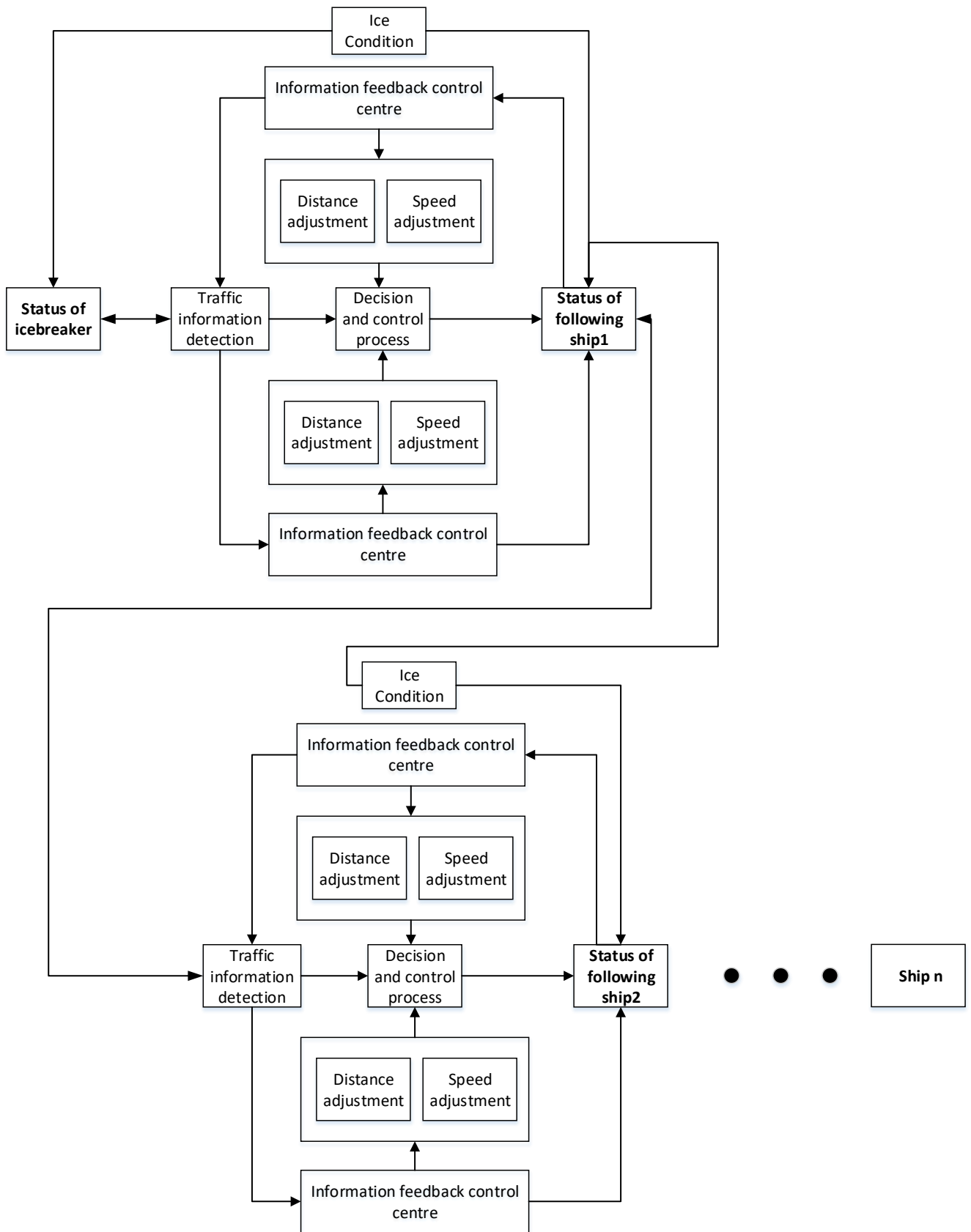
Figure 4. Following diagram of ships following in ice-covered waters

3.2 Model considering the effects of situational awareness and environmental conditions

In this section, the proposed model originates from the concept of OV models (Bando et al. 1995) where the OV of each vehicle is estimated based on the distance to the preceding vehicle and relative speed acceleration. In the OV model, the basic factors of kinematics including speed, displacement and accelerated velocity are used. All these factors belong to the category of object movement except the environmental factors. Thus, the OV model can be used not only in road traffic analysis, but also in marine traffic modelling, along with ice conditions. In this research, there is the change of the OV models, considering the situational awareness of the crew, linking the vigilance with respect to other vessels in convoy and environmental conditions. This leads to the early enough speed adjustments to keep the desired minimal safe distance between the own and preceding ship. The change of the OV models can be expressed as the OVI model. The model takes the following form (Zhang et al., 2019):

$$\frac{dv_n(t)}{d(t)} = \alpha[V(\Delta x_n(t)) - v_n(t)] - a_i \tag{6}$$

where α represents the sensitivity coefficient of the officer of the watch on board own ship; $v_n(t)$ is the speed of ship n at time t, $\Delta x_n(t) = x_{n+1}(t) - x_n(t)$ represents the distance between the own ship and preceding ship, a_i represents the acceleration of the icebreaker that is influenced by ice, and $V(\Delta x_n(t))$ represents the optimal speed, as shown in Eq. (7).

$$V(\Delta x_n(t)) = v_{\max}[\tanh(\Delta x_n(t) - d_c) + \tanh(d_c)]/2 \tag{7}$$

where $v_{\max}$ represents the maximum speed and d_c is the safe distance.

According to Newton's second law, the acceleration a_i caused by ice on the icebreaker is expressed as Eq. (8).

$$a_i = \frac{R_{BR}}{M} \tag{8}$$

where M represents the mass of the ship and R_{BR} represents the ice resistance.

To calculate the ice resistance the following semi-empirical formula is adopted (Lindqvist G, 1989).

$$R_{BR} = 1.8\sigma_f^{0.853} h^{1.656} v^{0.259} M^{0.147} W^{-0.099} \tag{9}$$

where σ_f represents the bending strength of the ice, h represents the ice thickness, v represents the ship speed, M stands for the ship mass, and W is the ship width. The bending strength of ice is about 500 kPa in the Baltic Sea (Wang and Zhang, 2010). The mass of a ship can be expressed by Eq. (10) (Scharrer et al. 2002).

$$Mg = \rho_w g V_d = 1 \times 10^3 g \times L \times W \times D \times C_B \tag{10}$$

where L and W represent the length and width of the ship, respectively, D represents its draft, C_B is the block coefficient (Schneekluth and Bertram, 1998), ρ_w is the density of water, and V_d is the volume of the displacement of the ship, which is calculated as the light displacement (equal to the gross registered tonnage minus the gross deadweight tonnage) (Watson, 1998).

3.3 BLI-OVCM model

Peng et al. (2016) proposed an optimal velocity change with memory (OVCM) model. It can be determined from the model that when the current vehicle's speed increases within a certain period of time, the vehicle is accelerating, and vice versa. Sun et al. (2012) proposed an optimal velocity model that considers the backward-looking effect or backward-looking and velocity difference (BLVD).

The speed and distance of the icebreaker and following ship will be limited by the following. Firstly, the current ship's speed should match that of the preceding ship. Secondly, when the distance between the ships is too large, the following ship is easily hindered by broken floe-ice in the channel. In severe cases, ice may cause hull damage. Hence, the following ship should speed up to reduce the gap with the current ship. Finally, when an icebreaker suddenly stops, it should maintain a sufficient distance between ships to prevent collisions. In Figure 5, S_P, S_C and S_F represent the statuses of the preceding ship, current ship and following ship, respectively. A diagram of the communication conditions of these ships is given in Figure 5.
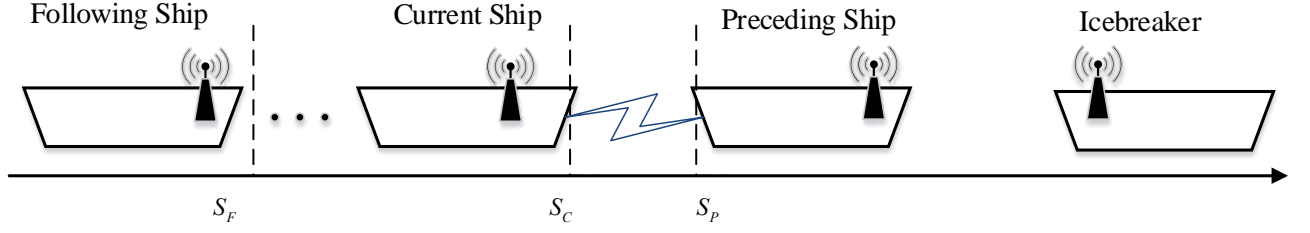
Figure 5. Diagram of multi-ship communication

Unlike the study of road traffic, a fleet needs to take account of the ability of the ships to navigate through ice. With the help of the communication network, the crews can share detailed navigation information between the ships. Thus, it is possible to have a general memory of the navigational conditions of the fleet. According to the maritime conditions, a corresponding navigation strategy will be made over a period of time, then the crews can make a corresponding adjustment in advance. With the development of communication, the ships' officers can receive much information through ship-ship communication. $pV_F(\Delta x_n(t))$ represents the effect from the leading ship to the following ship, meanwhile, $(1-p)V_B(\Delta x_{n-1}(t))$ represents the effect from the following ship to the leading ship. The parameter γ is defined to denote the intensity of the communication signal, and τ is the memory time step. When the optimal speed of the ship is higher than the optimal speed at a previous time, the ship is accelerating. Combining the effects of the OVCM model, the BLVD model and ice conditions, this study proposes a new multi-ship following model that can be applied to sea-ice environments by considering backward-looking, ice resistant and optimal velocity change with memory (BLI-OVCM). It represents the following behaviour of a network of ships. Its equation is shown as Eq. (11).

$$v_n(t+T) = pV_F(\Delta x_n(t)) + (1-p)V_B(\Delta x_{n-1}(t)) + \lambda \Delta v_n(t)T + \gamma[V(\Delta x_n(t)) - V(\Delta x_n(t-\tau))]T - a_iT \quad (11)$$

where $0.5 \le p \le 1$ represents the attention given by the current ship's crews to the preceding ship, and $1-p$ represents the degree of influence of the following ship on the current ship. The crews can receive information on the velocity difference and distance at time t, then adjust the sailing velocity to fit the optimal velocity. This takes a certain amount of reaction time T. During the voyage of the fleet, the current ship pays more attention to the preceding ship than the following ship, which is also in line with the actual environment. $V(\Delta x_n(t)) - V(\Delta x_n(t-\tau))$ represents the difference in optimal speed which varies with time, where τ is the memory time step, λ is sensitivity coefficient of velocity difference and γ is the sensitivity coefficient of optimal speed as a function of the memory time step. $V_F(\Delta x_n(t))$

is the optimal speed from forward observation, and $V_B(\Delta x_{n-1}(t))$ represents the optimal speed for backward observation, $a_i = \dfrac{R_{BR}}{M}$ is drag acceleration due to the impact of ice on icebreakers, where M represents the mass of the ship, and R_{BR} represents the ice resistance. According to Eq. (7), $V_F(\Delta x_n(t))$ and $V_B(\Delta x_{n-1}(t))$ can be expressed as Eq. (12) and Eq. (13).

$$V_F(\Delta x_n(t)) = v_{max}[\tanh(\Delta x_n(t) - d_c) + \tanh(d_c)]/2 \tag{12}$$

$$V_B(\Delta x_{n-1}(t)) = v_{max}[\tanh(\Delta x_{n-1}(t) - d_c) + \tanh(d_c)]/2 \tag{13}$$

where $\Delta x_{n-1}(t) = x_n(t) - x_{n-1}(t)$ is the distance between the current and following ships, d_c represents the safe distance between two ships. Introducing the optimal speed of the fleet should take account of the following two points: firstly, the optimum speed is sensitive to the safe distance; secondly, the optimal speed is dependent on the environment of the route.

Due to the delay time in the BLI-OVCM model, it is not applicable to stability analysis and simulation verification. At the same time, the coefficient of the exponential term for velocity in the calculation of the ice resistance acceleration to the ship is not an integer, which is not suitable to stability analysis of the model. In the stability analysis, the acceleration is more intuitive than the speed. Therefore, the left side of Eq. (11) is extended by Taylor's theorem.

$$v_n(t+T) = v_n(t) + Ta_n(t) \tag{14}$$

where $v_n(t)$ is the speed of ship n at time t, and $a_n(t)$ is the acceleration of ship n at time t. This takes a certain amount of reaction time T.

The equation for the acceleration obtained by Eq. (11) and Eq. (12) is shown as Eq. (13).

$$\frac{dv_n(t)}{d(t)} = \frac{1}{T}[pV_F(\Delta x_n(t)) + (1-p)V_B(\Delta x_{n-1}(t)) - v_n(t)] + \lambda \Delta v_n(t) + \gamma[V(\Delta x_n(t)) - V(\Delta x_n(t-\tau))] - a_i \tag{15}$$

Let $\alpha=\dfrac{1}{T}$ be the sensitivity coefficient of the reaction time. The slower the reaction time of the crew, the smaller the sensitivity coefficient. A higher sensitivity coefficient means better stability. Substituting $\alpha=\dfrac{1}{T}$ into Eq. (15) results in Eq. (16).

$$\frac{dv_n(t)}{d(t)} = \alpha[pV_F(\Delta x_n(t)) + (1-p)V_B(\Delta x_{n-1}(t)) - v_n(t)] + \lambda\Delta v_n(t) + \gamma[V(\Delta x_n(t)) - V(\Delta x_n(t-\tau))] - a_i \tag{16}$$

At the same time, for the sake of simplicity, a Taylor series expansion of the variable $\Delta x_n(t-\tau)$ can be obtained as shown in Eq. (17).

$$\Delta x_n(t-\tau) = \Delta x_n(t) - \tau\frac{d\Delta x_n(t)}{dt} = \Delta x_n(t) - \tau\Delta v_n(t) \tag{17}$$

Moreover, the linear term $V(\Delta x_n(t-\tau))$ can be deduced as follows:

$$V(\Delta x_n(t-\tau)) = V(\Delta x_n(t)) - \tau\Delta v_n(t)V'(\Delta x_n(t)) \tag{18}$$

At this point, Eq. (16) can be rewritten as:

$$\frac{dv_n(t)}{d(t)} = \alpha[pV_F(\Delta x_n(t)) + (1-p)V_B(\Delta x_{n-1}(t)) - v_n(t)] + \lambda\Delta v_n(t) + \gamma\tau\Delta v_n(t)V'(\Delta x_n(t)) - a_i \tag{19}$$

The resistance acceleration of ice $a_i = \dfrac{R_{BR}}{M}$, where R_{BR} is as shown in equation Eq. (9). To simplify the stability analysis, the speed exponential coefficient R_{BR} is enlarged from less than 1 to 1 as an integer. Here, the greater value of influence of ice represents a stricter criterion for stability analysis. In stability analysis, the expression of a_i is $a_i = \beta v$, where,

$$\beta = \frac{1.8\sigma_f^{0.853}h^{1.656}M^{0.147}B^{-0.099}}{M}.$$

The fleet's voyage is affected by the behaviours of the preceding ship, the following ship and the ice conditions. Using radiotelephony communication, pre-reaction of the crews helps the fleet sail more steadily. Next, the stability of the proposed model will be analysed.

4. MODEL STABILITY ANALYSIS AND VALIDATION

4.1 Stability analysis

The disturbance method was adopted for stability analysis of the ship following model (BLI-OVCM). Small disturbances were made to the following fleet. For example, when a following ship encounters increased ice resistance, its status changes (such as its velocity), thus its steady navigational state is expected to change – being disturbed. Then, the influence of this disturbance is modelled as follows.

Firstly, assuming the icebreaker is in the process of continuous icebreaking, the fleet maintains a constant distance d between two consecutive ships. At the same time, the fleet always maintains an optimal speed $pV_F(d) + (1-p)V_B(d)$, and the position of each ship in the fleet can be calculated by Eq. (20).

$$x_n^0(t) = dn + (pV_F(d) + (1-p)V_B(d))t \tag{20}$$

When ship n encounters floating ice, it may deviate from its stable state. The parameter t represents the time of ship navigation, and the parameter d equals the distance between two consecutive ships plus the ship length. According to Euler's formula, the kinematics formula can be expressed as $y_n(t) = e^{ikn+zt}$ while applying a small disturbance. Then, the position under the disturbance of ship n is obtained as follows.

$$x_n(t) = x_n^0(t) + y_n(t) \tag{21}$$

where $y_n(t) = x_n(t) - x_n^0(t)$. To calculate the first-order derivative of $y_n(t)$,

$$\frac{dy_n(t)}{dt} = \frac{dx_n(t)}{dt} - (pV_F(d) + (1-p)V_B(d)) \tag{22}$$

The derivative of Eq. (22) is calculated to obtain $\dfrac{d^2 y_n(t)}{d^2 t} = \dfrac{dv_n(t)}{dt}$. Letting $\Delta y_n(t) = y_{n+1}(t) - y_n(t)$, the head distance of the ships is calculated as:

$$\Delta x_n(t) = b + \Delta y_n(t) \tag{23}$$

16

Substituting the above linear results into the proposed model, the relevant differential equations are obtained as follows:

$$\frac{d^2 y_n(t)}{d^2 t} = \alpha[pV_F^{'}(d)\Delta y_n + (1-p)V_B^{'}(d)\Delta y_{n-1} - \frac{dy_n(t)}{dt}] + \lambda \frac{d\Delta y_n(t)}{dt} + \gamma\tau V_F^{'}(\Delta x_n(t))\frac{d\Delta y_n(t)}{dt} - \beta\frac{dy_n(t)}{dt}$$

(24)

where $V_F^{'}(d) = \frac{dV_F(\Delta x_n(t))}{d\Delta x_n(t)} | \Delta x_n(t) = d$ and $V_B^{'}(d) = \frac{dV_B(\Delta x_{n-1}(t))}{d\Delta x_{n-1}(t)} | \Delta x_{n-1}(t) = d$.

From the disturbance $y_n(t) = e^{ikn+zt}$, the following is obtained:

$$\frac{dy_n(t)}{dt} = Ze^{ikn+zt}$$

(25)

$$\frac{d^2 y_n(t)}{d^2 t} = Z^2 e^{ikn+zt}$$

(26)

$$\Delta y_n(t) = e^{ikn+zt}\left(e^{ik} - 1\right)$$

(27)

Substituting Eq. (25), Eq. (26) and Eq. (27) into Eq. (24), the following results are obtained:

$$Z^2 = \alpha[pV_F^{'}(d)(e^{ik}-1) + (1-p)V_B^{'}(d)(1-e^{ik}) - Z] + \lambda Z(e^{ik}-1) + \gamma\tau V_F^{'}(d)Z\left(e^{ik}-1\right) - \beta Z$$

(28)

To solve Eq. (28), Taylor series expansion is carried out for e^{ik} and e^{-ik} , respectively: $e^{ik} = 1 + ik + \frac{ik^2}{2}$, $e^{-ik} = 1 - ik + \frac{ik^2}{2}$. Substituting e^{ik} and e^{-ik} into Eq. (28) and expanding the parameter Z with Taylor series, then $Z = Z_1 ik + Z_2 ik^2 + ...$ is obtained. Therefore, Taylor series expansions of the first- and second-order are obtained as per Eq. (29) and Eq. (30).

$$Z_1 = \frac{pV_F^{'}(d) + (1-p)V_B^{'}(d)}{\frac{\beta}{\alpha} + 1}$$

(29)

$$Z_2 = \frac{pV_F^{'}(d)-(1-p)V_B^{'}(d)}{2(\frac{\beta}{\alpha}+1)} + \frac{[\lambda Z_1 - Z_1^2 + \gamma\tau V_F^{'}(d)Z_1]}{\alpha\left(\frac{\beta}{\alpha}+1\right)} \tag{30}$$

If $Z_2 < 0$, the fleet will be in an unstable state (Tang et al., 2009); otherwise, if $Z_2 > 0$, then the fleet will be in a state of stability. The stability curve can be obtained by Eq. (31) and the following process:

$$\alpha = \frac{2[-\lambda Z_1 + Z_1^2 + \gamma\tau V_F^{'}(d)Z_1]}{pV_F^{'}(d)-(1-p)V_B^{'}(d)} \tag{31}$$

Where $Z_2 > 0$, the fleet will be in a state of stability. Thus, the condition of $\alpha > \frac{2[>\lambda Z_1 + Z_1^2 + \gamma\tau V_F^{'}(d)Z_1]}{pV_F^{'}(d)-(1-p)V_B^{'}(d)}$ should be satisfied.

Let

$$e = 2[-\lambda[pV_F^{'}(d)+(1-p)V_B^{'}(d)] + \gamma\tau V_F^{'}(d)[pV_F^{'}(d)+(1-p)V_B^{'}(d)]] \tag{32}$$

$$c = 2[pV_F^{'}(d)+(1-p)V_B^{'}(d)]^2 \tag{33}$$

$$s = pV_F^{'}(d)-(1-p)V_B^{'}(d) \tag{34}$$

Therefore, $\alpha > \dfrac{\dfrac{c}{(1+\frac{\beta}{\alpha})^2} + \dfrac{e}{1+\frac{\beta}{\alpha}}}{s}$ can be obtained. Finally, the solutions are:

$$\alpha_1 > \frac{-(2\beta-e-c)+\sqrt{(2\beta-e-c)^2-4(\beta^2 s-\beta e)}}{2} \tag{35}$$

$$\alpha_2 > \frac{-(2\beta-e-c)-\sqrt{(2\beta-e-c)^2-4(\beta^2 s-\beta e)}}{2} \tag{36}$$

Due to the stability constraints of non-negative numbers, α_1 is the final solution. Similarly, the stability conditions of OVI can be obtained as per Eq. (37).

$$\alpha' > -\left(\beta - V_F'(d)\right) + \sqrt{\left(\beta - V_F'(d)\right)^2 - \beta^2} \qquad (37)$$

4.2 Validation

This section analyses the simulation of stability of both the OVI and BLI-OVCM models. In this study, AIS and icebreaker convoy data from operations in the Baltic Sea from 1–11 March 2011 was used. This period was in late winter when sea-ice conditions were severe. For validation, the icebreaker *Fennica* was followed by two ships using real data from March 12, 2011. When the BLI-OVCM model is drawn, the values of the coefficients, $p = 0.9, \lambda = 0.2, \tau = 0.2, \gamma = 0.2$, are used, which are determined by experience. The effect of different parameter values will be discussed in Section 4.3. In particular, when $p = 1, \lambda = 0, \tau = 0, \gamma = 0$, the model is transformed into the OVI model form. On the basis of neutral stability conditions, the stability curves of ship spacing and crews' response sensitivity can be obtained, as shown in Figure 6, which is based on Eqs. (35) and (37). In this way, the stable and unstable area are also determined by the equations.
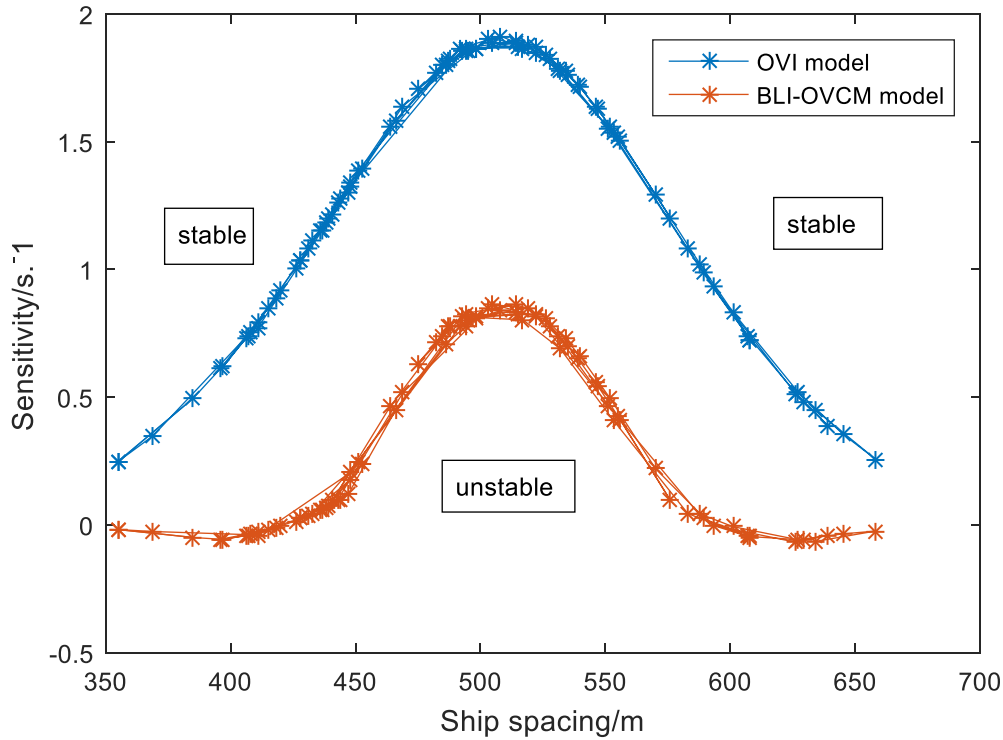

Figure 6. Comparison of the neutral stability curves of the models

The whole area in Figure 6 is divided into two parts by the neutral stability curve. The area above the neutral stability curve is the stable area, and the area underneath the neutral stability curve is the unstable area. In unstable areas, when a ship is disturbed, the stability of the following ship decreases, which can easily lead to a collision. Consequently, the ship will be forced to stop and may become frozen in the ice. Compared to the OVI model, the stability of the proposed BLI-OVCM model is greatly improved, which is conducive to the stable operation of fleets in ice-covered waters. Moreover, it can be applied as a theoretical basis for software simulation.

4.3 Parameter discussion

Different model parameters have different effects on the model. Discussion of the parameters can help us find suitable parameters for model simulation and understand their influence on fleet stability.

Firstly, parameter p of the multi-ship following model is discussed, which represents the effect of the preceding ship on the current ship. Generally speaking, the preceding ship will have a greater impact on the current ship than the following ship. Therefore, the value of parameter p is between 0.5 and 1. The influence of p on the stability of a fleet's voyage is shown in Figure 7.
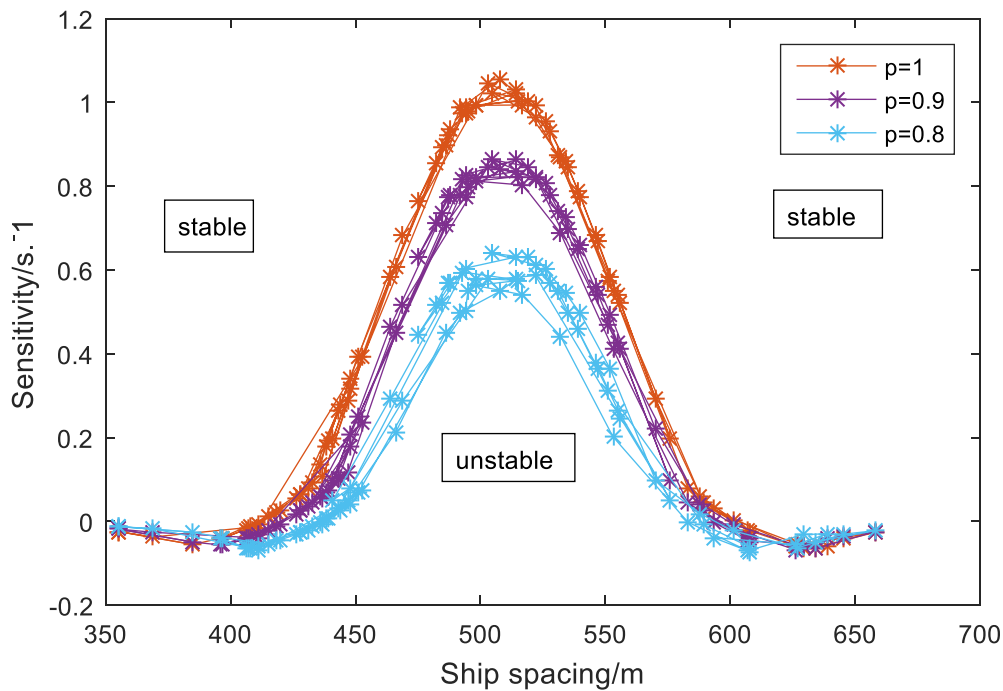

Figure 7. Stability curves with different values of parameter p

It can be seen from Figure 7 that as parameter p decreases, the stability increases. This indicates that the effect of the following ship on the current ship is positive to improving the stability.

Parameter λ represents the sensitivity of the current ship from the speed difference of the preceding ship. The effect of λ on the stability of a fleet's voyage is shown in Figure 8.
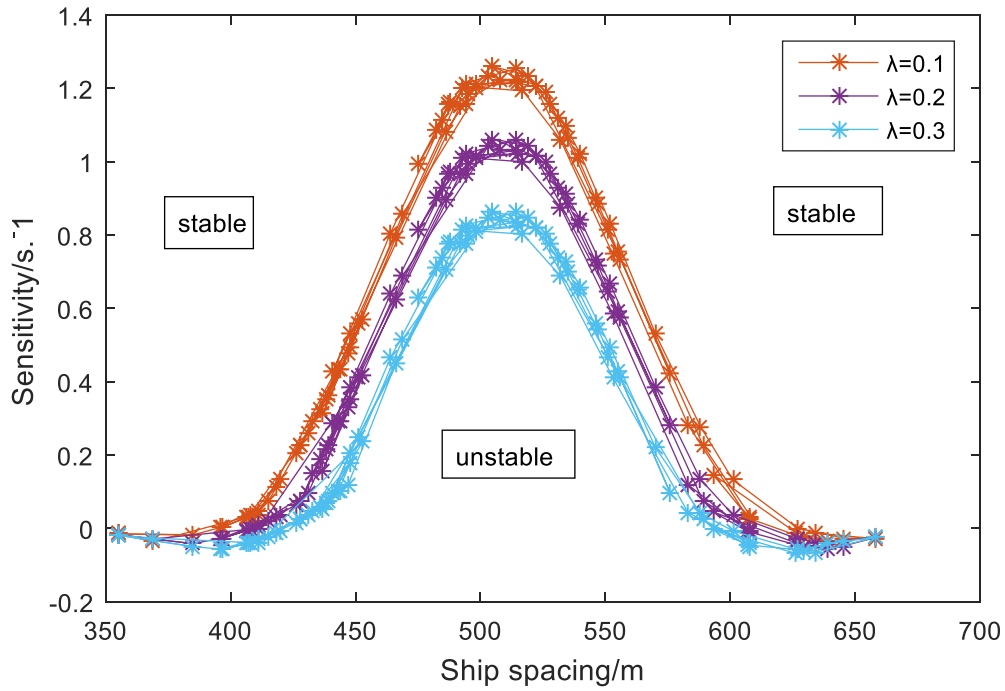

Figure 8. Stability curve with different values of parameter λ

It can be seen from Figure 8 that the stability continuously improves as parameter λ increases, meaning that the stability can be improved by paying more attention to the speed difference between the current and preceding ships.

Parameters τ and γ also need to be investigated; τ represents a memory step and γ is a sensitivity coefficient of the optimal speed memory associated with the preceding ship. These two parameters can be replaced by each other. If only considering parameter τ, its effects on the stability of the ship are as shown in Figure 9.
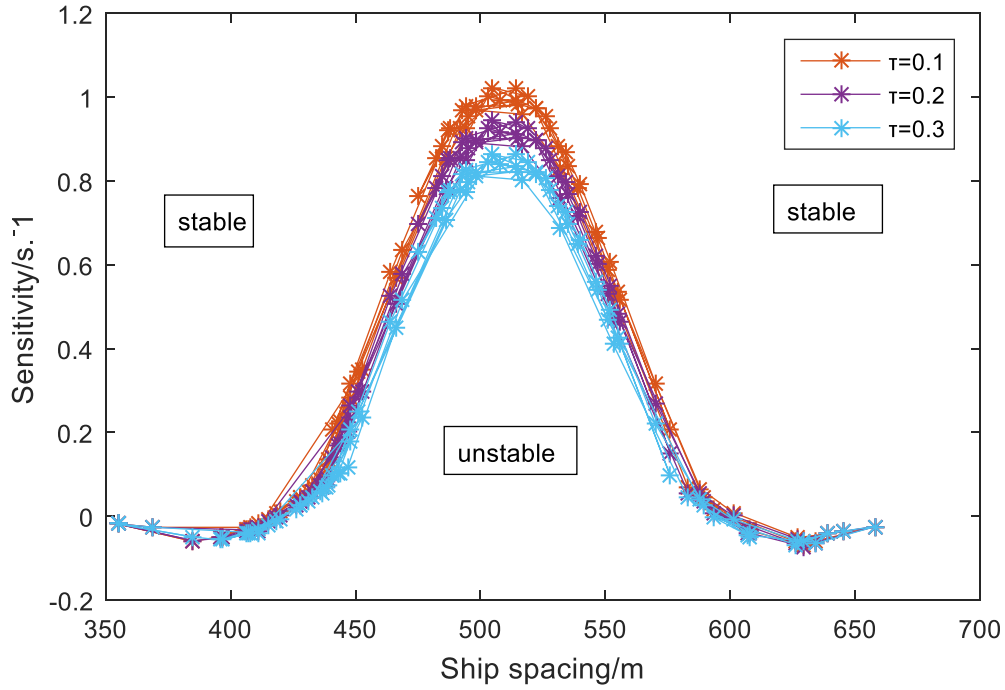
Figure 9. Stability curve with different values of parameter τ

It can be seen from Figure 9 that the stability of the fleet continuously improves as parameter τ increases, meaning that the better the memory effect, the higher the stability of the ships.

4.4 Simulation verification and comparison

This section compares the modelled results with actual data. It also compares the simulation speed of the OVI and BLI-OVCM models. In order to verify the models, we used three performance measures, namely, the correlation coefficient (R), mean absolute percentage error ($MAPE$) and root-mean-square error ($RMSE$). The larger the correlation coefficient R, the smaller $MAPE$ and $RMSE$, which indicates better model performance. These three parameters are given as follows:
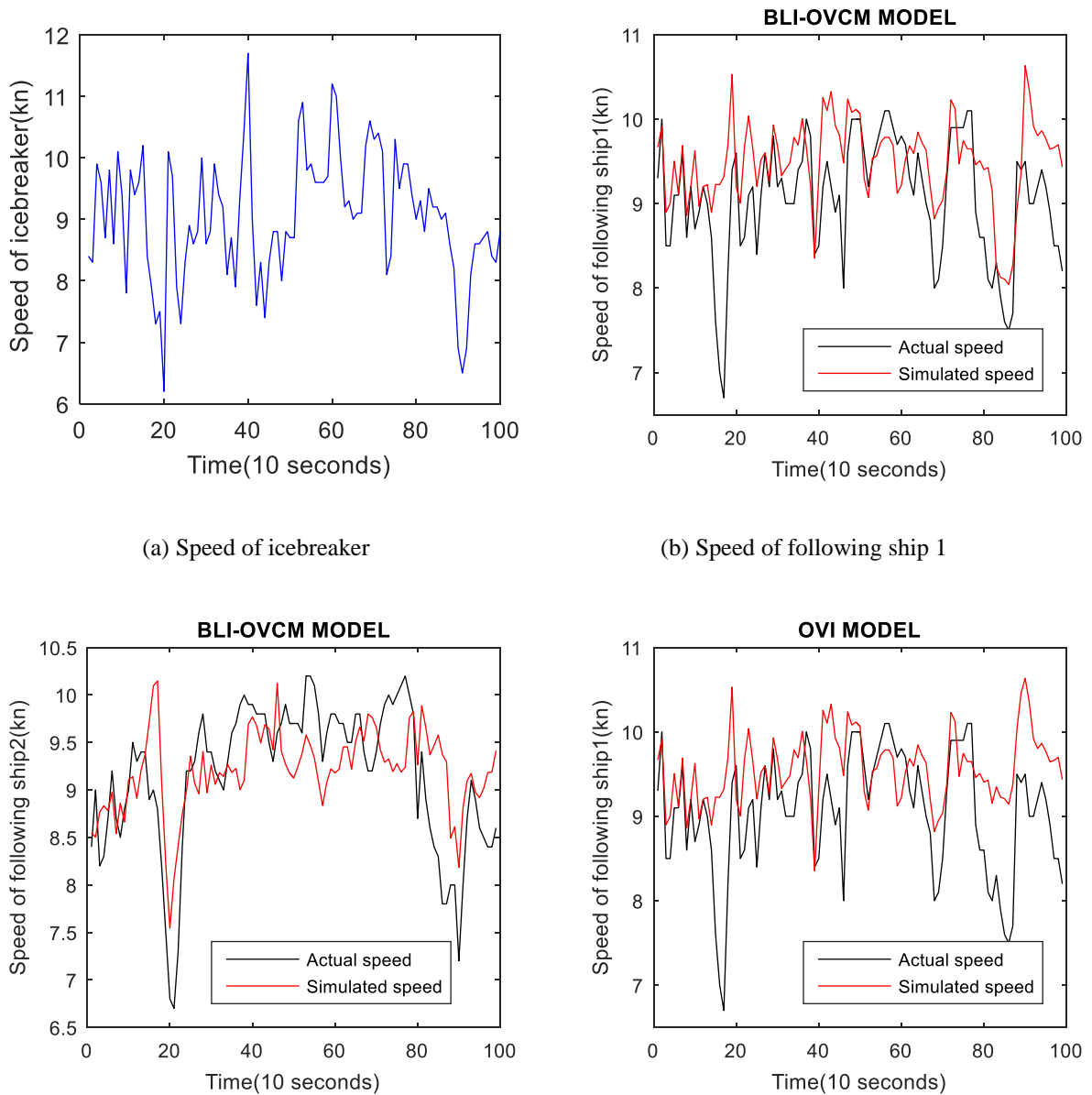
$$R = \frac{\sum_{i=1}^{N}\left(v_{model,i} - \overline{v}_{model,i}\right)\left(v_{obs,i} - \overline{v}_{obs,i}\right)}{\sqrt{\sum_{i=1}^{N}\left(v_{model,i} - \overline{v}_{model,i}\right)^{2}\sum_{i=1}^{N}\left(v_{obs,i} - \overline{v}_{obs,i}\right)^{2}}} \tag{38}$$

$$MAPE = \frac{1}{N}\sum_{i=1}^{N}\frac{\left|v_{model,i} - v_{obs,i}\right|}{v_{obs,i}} \times 100\%$$

(39)

$$RMSE = \sqrt{\frac{\sum_{i=1}^{N}\left(v_{\mathrm{model},i} - v_{obs,i}\right)^{2}}{N-1}} \qquad (40)$$

In the above equations, N represents the sample size; $v_{obs,i}$ represents the ship speed at time i; and $v_{\mathrm{model},i}$ represents the simulated ship speed at time i.

Next, a comparison of the two models in a multi-ship following scenario is conducted. Simulation of the inter-ship distance by the new model is compared with actual data. As shown in Figure 9, the icebreaker is the *Fennica* and the time period is from 20:52:30 to 22:22:00, 12 March 2011.
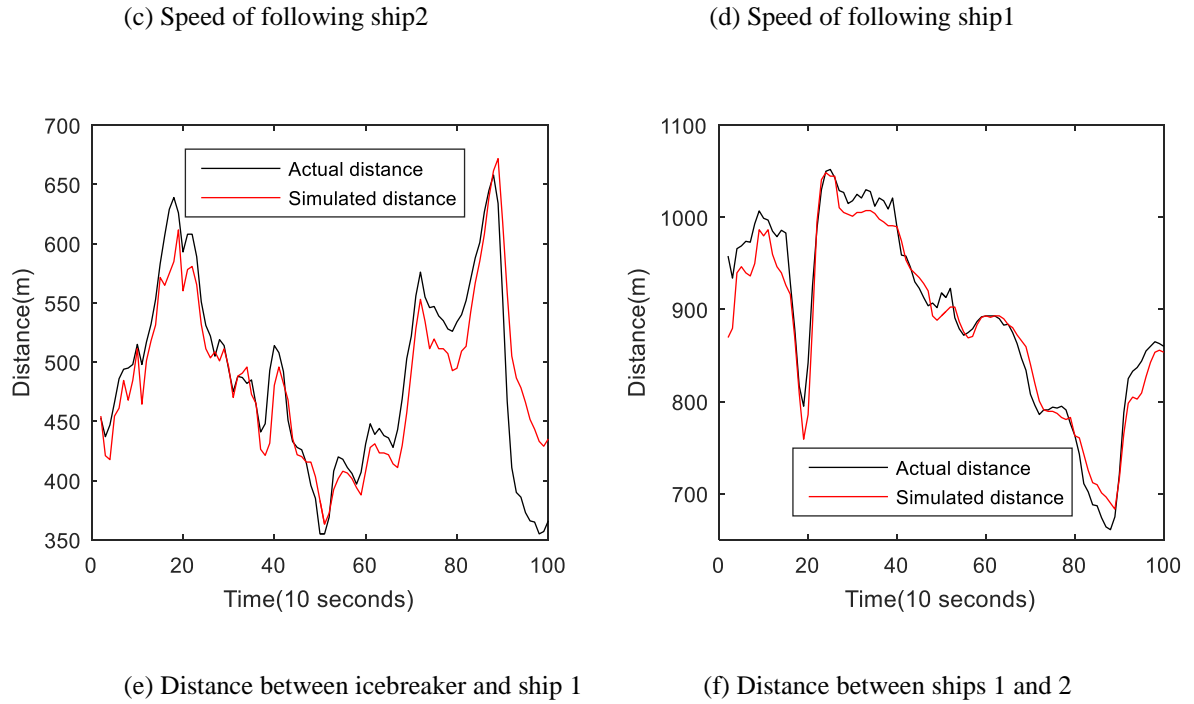

(a) Speed of icebreaker

(b) Speed of following ship 1

(e) Distance between icebreaker and ship 1

(f) Distance between ships 1 and 2

Figure 10. Comparison of actual navigation data with simulations by the two proposed models

Firstly, the error analysis of the data is illustrated in Figure 10, with the error results shown in Tables 2 and 3. The OVI model represents the following behaviour of a normal ship and does not consider the effect of the network. The proposed model considers additional factors and provides better results than the optimal velocity approach. It is logical that the greater the number of ship observations used, the better the parameter calibration. Furthermore, the method is superior in that it is possible to estimate the source of the parameters. Figure 10 (a) shows the speed of the icebreaker, which the following ship follows by varying its speed. Figure 10 (b) shows the estimated and observed speed data for following ship 1. Over time, the estimated speed becomes more consistent with the observed speed. The estimated values in Figure 10 (b) show better performance than those in Figure 10 (d).

Table 2. Evaluation of simulated speed

Icebreaker (*Fennica*)	R	MAPE	RMSE (knots)
Following ship 1 (new model)	0.7723	6.55%	0.7352
Following ship 1 (OVI model)	0.5918	7.36%	0.8080
Following ship 2 (new model)	0.8098	5.69%	0.6119

Table 3. Evaluation of simulated distance

Icebreaker (*Fennica*)	R	MAPE	RMSE (m)
Following ship 1 (new model)	0.9791	2.04%	23.3228
Following ship 2 (new model)	0.8921	5.76%	35.6704

From Table 2, the R value of the new model (0.7723), is obviously greater than that of the OVI model (0.5918), while the $MAPE$ and $RMSE$ of the proposed model (6.55% and 0.7352, respectively) are smaller than those of the OVI model (7.36% and 0.8080). Table 3 represents the evaluation of simulated distance, where the R-values of following ship 1 and following ship 2 are 0.9791 and 0.8921. The larger the R-value, the better performance of the simulation. As the $MAPE$ and $RMSE$ show, the simulated distances have smaller errors than the real distances. The deviation in $MAPE$ is around 6%, while that of the $RMSE$ is around 36 m; both deviations are small. Although there is still some deviation, the proposed model can be considered to simulate the distance of the following ship in sea-ice and communication conditions described in Section 3.2 reasonably well. Here, the R-value represents the correlation between the simulated and actual values. It demonstrates that the proposed model not only performs better in terms of stability but also provides a lower deviation in the numerical simulation. Moreover, the R-values indicate a stronger correlation and lower error. This demonstrates that the proposed model can enhance safe navigation by maintaining stable sailing at safe speeds and distances, thereby reducing the risk of collisions between ships in the fleet.

5. CONCLUSIONS

In ice-covered water areas, the study of ship following models is of great significance for enhancing the understanding of polar shipping risk and improving navigational technology. In this paper, a multi-ship following model was constructed to represent the following behaviour of ships under the conditions of communication. This facilitates more stable navigation by considering the preceding and following ships in a fleet. Due to difficulties in experimentation and data collection, simulated data was used to investigate the safe inter-ship distances and maximum speeds of ships navigating areas of sea-ice in comparison with real data. In the process of building the model, the ice conditions were taken into account, which is based on the impact of ice resistance on the impeding acceleration of the icebreaker. The model was designed for icebreaker convoy operations and the maximum convoy speed was briefly analysed. In addition, stability analysis of the model was also carried out. The influences of different coefficients on stability were analysed. As a result, the model can be used to improve the navigation stability of fleets in ice-covered waters. It can be applied as a theoretical basis for software simulation.

In addition, the proposed model can be used for studying following behaviours of surface autonomous vessels.

The developed model takes ice conditions into consideration but does not fully consider the influences of factors such as winds and currents. Therefore, the model could be further improved by considering such factors to provide more accurate estimation of stability and safety. In addition, how this model supports surface autonomous ships' navigational operations in the polar region will be studied in the next step.

ACKNOWLEDGEMENTS

REFERENCES

Bole A. G. (Alan G.), Alan Wall, and Andy. Norris. 2014. Radar and ARPA Manual : Radar, AIS and Target Tracking for Marine Radar Users, Third Edition. Butterworth-Heinemann.

Bando M., Hasebe K., Nakayama A., Shibata A., Sugiyama Y., 1995. Dynamical model of traffic congestion and numerical simulation. Physical Review E Statistical Physics Plasmas Fluids & Related Interdisciplinary Topics, 51(2), 1035.

Cheng L. this is the 1.0 Age of Chinese Smart Ship：Shipping newspaper in china [DB/OL].[2019-9-23]: https://www.imarine.cn/article-8124-1.html.

Fu S., Zhang D., Montewka J., Zio E., Yan X.P. 2018. A Quantitative Approach for Risk Assessment of a Ship Stuck in Ice in Arctic Waters. Safety Science 107 (August): 145–54. https://doi.org/10.1016/J.SSCI.2017.07.001.

Goerlandt F., Montewka J., Zhang W., Kujala P.. 2017. An Analysis of Ship Escort and Convoy Operations in Ice Conditions. Safety Science 95: 198–209.

Haapala J., Lönnroth N., Stössel A. 2005. A Numerical Study of Open Water Formation in Sea Ice. Journal of Geophysical Research: Oceans 110 (C09011): 1–17.

Juurmaa K., Heideman T., Uusikallio A. 1998. Influence of Ice Compression on Feasible Navigation on the Northern Sea Route.Part II. 110. I.1.8.

Kotilainen M., Vanhatalo J., Suominen M., Kujala P. 2017. Predicting Ice-Induced Load Amplitudes on

Ship Bow Conditional on Ice Thickness and Ship Speed in the Baltic Sea. Cold Regions Science and Technology 135 (March): 116–26.

Kubat I. 2012. Quantifying Ice Pressure Conditions and Predicting the Risk of Ship Besetting. In International Conference and Exhibition on Performance of Ships and Structures in Ice 2012 (ICETECH 2012). Society of Naval Architects and Marine Engineers (SNAME).

Kubat I., Hossein B., Mohamed S. 2013. Analysis of Besetting Incidents in Frobisher Bay during 2012 Shipping Season. In Proceeding of International Conference on Port and Ocean Engineering Undere Arctic Conditions (POAC). Espoo, Finland.

Kubat I., Captain D.F., Mohamed S. 2015. Snow and Ice-Related Hazards, Risks and Disasters. Snow and Ice-Related Hazards, Risks and Disasters. Elsevier. https://doi.org/10.1016/B978-0-12-394849-6.00018-4.

Kujala P., Sankar A. 2012. Statistical Analysis of Ice Crushing Pressures on a Ship's Hull during Hull–Ice Interaction. Cold Regions Science and Technology 70: 1–11.

K. Kim, J. Jeong, and B. Lee, 2017. Study on the Analysis of Near-Miss Ship Collisions Using Logistic Regression, J. Adv. Comput. Intell. Intell. Inform., Vol.21, No.3, 467-473.

Kum S., Bekir S. 2015. A Root Cause Analysis for Arctic Marine Accidents from 1993 to 2011. Safety Science 74: 206–20.

Lehtiranta J., Lensu M., Haapala J. 2012. Ice Model Validation on Local Scale. Helsinki, Finland: Finnish Meteorological Institute.

Lensu M., Iiro K. 2017. Inventory of Ice Performance for Baltic Sea IA Super Traffic 2007-2016. N/A. Winter Navigation Research Board. Helsinki.

Liikennevirasto. 2017. Finland's Winter Navigation. Instructions for Winter Navigation Operators. Helsinki, Finland.

Lindqvist G., 1989. A straightforward method for calculation of ice resistance of ships. In: Proc. 10th Int. Conf. Port and Ocean Engineering Under Arctic Conditions (POAC 1989). Luleå, Sweden.

Löptien U., Dietze H. 2014. Sea Ice in the Baltic Sea – Revisiting BASIS Ice, a Historical Data Set Covering the Period. Earth Syst. Sci. Data 6: 367–74.

McCallum J．Safe speed in ice: an analysis of transit speed and ice decision numerals．Ship Safety Northern (AMNS)．Ottawa: Transport Canada, 1996．

Montewka J., Goerlandt F., Kujala P., Lensu M. 2015. Towards Probabilistic Models for the Prediction of a Ship Performance in Dynamic Ice. Cold Regions Science and Technology 112: 14–28.

Montewka J., Goerlandt F., Lensu M., Kuuliala L., Guinness R. 2019. Toward a Hybrid Model of Ship

Performance in Ice Suitable for Route Planning Purpose. Proceedings of the Institution of Mechanical Engineers, Part O: Journal of Risk and Reliability 233 (1): 18–34.

Peng G., Lu W., He H., 2016. Nonlinear analysis of a new car-following model accounting for the global average optimal velocity difference. Modern Physics Letters B, 30(27), 1650327-.

Ramos, M.A., Utne, I.B., Mosleh, A., 2019. Collision avoidance on maritime autonomous surface ships: Operators' tasks and human failure events. Safety Science, 116: 33-44.

Rolf J. Bye, Asbjørn L. Aalberg. Maritime navigation accidents and risk indicators: An exploratory statistical analysis using AIS data and accident reports. Reliability Engineering & System Safety, 2018, 176:174-186.

Rosenblad M., 2007. Increasing the Safety of Icebound Shipping – WP4 Operative Environment (Icebreaker Operations). Helsinki University of Technology, Espoo, Finland.

Schneekluth H., Bertram V. (1998). Ship design for efficiency and economy (Vol. 218). Oxford: Butterworth-Heinemann.

Scharrer M., Zhang L., Egge E.D., 2002. Collision calculations in naval design systems. Report Nr. ESS 2002.183. Hamburg: Germanischer Lloyd.

Sun D.H., Zhang J.C., Zhao M., Tian C. 2012. Effect of backward looking and velocity difference in an extended car following model. Journal of Sichuan University.

Tang T.Q., Huang H.J., Zhao S.G. An extended OV model with consideration of driver's memory. International Journal of Modern Physics B, 2009, 23(5):743-752.

Thombre S., Robert G., Chen L., Laura R., Heidi K., Janusz U., Zbigniew P., Juhani L., Philippe G. 2015. ESABALT Improvement of Situational Awareness in the Baltic with the Use of Crowdsourcing. TransNav, the International Journal on Marine Navigation and Safety of Sea Transportation 9 (2): 183–89.

Transport Canada. 2018. Arctic Ice Regime Shipping System (AIRSS) Standard. Ottawa.

Valdez Banda O.A., Goerlandt F., Kuzmin V., Kujala P., Montewka P. 2016. Risk Management Model of Winter Navigation Operations. Marine Pollution Bulletin 108 (1–2).

Valdez Banda O.A., Goerlandt F., Montewka J., Kujala P. 2015. Winter Navigation at the Baltic Sea: An Analysis of Accidents Occurred during Winters 2002-2003 & 2009-2013. In Safety and Reliability: Methodology and Applications - Proceedings of the European Safety and Reliability Conference, ESREL 2014, 83–92.

Valdez Banda O. A., Goerlandt F., Montewka J., and Kujala P. 2015. A Risk Analysis of Winter Navigation in Finnish Sea Areas. Accident Analysis & Prevention 79 (June): 100–116.

Wang, L., Liu, Q., Dong, S., 2019. Effectiveness assessment of ship navigation safety countermeasures

using fuzzy cognitive maps. Safety Science, 117:352-364.

Watson D. G. M., 1998. Practical ship design. Elsevier Ocean Engineering Book.

Wawruch R. 2017. Ability to Test Shipboard Automatic Identification System Instability and Inaccuracy on Simulation Devices. Scientific Journals of the Maritime University of Szczecin-Zeszyty Naukowe Akademii Morskiej W Szczecinie.

Yim J.B., Kim D.S., Park D.J. 2018. Modeling Perceived Collision Risk in Vessel Encounter Situations. Ocean Engineering 166 (October): 64–75.

Wang Y W., Zhang D X. 2010. Analysis and Suggestions about Ice Class Definition. Naval Architecture and Ocean Engineering (4), 54-58.

Zhang L., Meng Q., 2019. Probabilistic ship domain with applications to ship collision risk assessment. Ocean Engineering, 186: 106-130.

Zhang M., Zhang D., Fu S., Yan X., Goncharov V. 2017. Safe distance modeling for ship escort operations in arctic ice-covered waters. Ocean Engineering, 146, 202-216.

Zhang, W., Goerlandt, F., Montewka, J., & Kujala, P., 2015. A method for detecting possible near miss ship collisions from ais data. Ocean Engineering, 107, 60-69.

Zhang W., Goerlandt F., Kujala P., Qi Y. 2018. A coupled kinematics model for icebreaker escort operations in ice-covered waters. Ocean Engineering, 167:317-333.

Zhang W., Zou Z., Goerlandt F., Qi Y., and Kujala P. 2019. A Multi-Ship Following Model for Icebreaker Convoy Operations in Ice-Covered Waters. Ocean Engineering 180 (May): 238–53.